Available online at www.sciencedirect.com
SCIENCE DIRECT®
Journal of Chromatography A, 1039 (2004) 13–21
JOURNAL OF CHROMATOGRAPHY A
www.elsevier.com/locate/chroma

Investigation of new chelation ion chromatography procedure to determine the surface composition of powdered metal oxide samples in the solid state

Brian C. Peebles*, Michael P. Setter

Department of Chemistry, John Carroll University, 20700 North Park Boulevard, University Heights, OH 44118, USA

Available online 27 February 2004

Abstract

Numerous tests have been conducted on the feasibility of characterizing the surfaces of metal oxide powders using HPLC. An in-line filter housing was modified to serve as a sample chamber to replace the sample loop. A gradient pump was used to gradually increase eluent acidity to find the conditions at which the surface of a metal oxide powder began to dissolve. The theoretical masses of surface monolayers of metal oxide powders were compared with the experimentally determined masses of dissolved material thought to be from the surface to test whether surface and bulk dissolution phenomena in acidic conditions are separable and quantifiable. A set of methods was tested that could first dissolve a metal oxide sample's surface, then separate and detect analyte species by chelation ion chromatography. Surface characterization by ion chromatography could be more cost-effective than existing methods, and reveal chemical properties of the sample where existing methods only give physical composition and properties.

Keywords: Chelation; Surface composition; Metal oxides

1. Introduction

The behavior of a powder often depends upon the composition of its surface. For example, only the surface of an atmospheric particulate interacts with other atmospheric components. Similarly in the field of heterogeneous catalysis, the surface of the catalyst holds the catalytically active sites. The battery industry also requires knowledge of both surface and interior compositions to determine the electrochemical behavior of a powder. The surface provides the reaction site, as in catalysts, but the interior provides the energy storage capacity.

Traditional compositional analysis of a powder yields a total composition, combining the surface with the interior. Since the amount of material in the interior is significantly greater than that at the surface, such a total analysis inherently biases the composition towards the interior, obscuring the significant surface chemistry. The potential discrepancy between surface and interior compositions poses a problem to the analytical chemist.

Techniques exist to probe surfaces of large-scale materials, but not of the sub-micrometer to 100 μm size particles typically found in powders. Without compositional information for these powders, there is an inherent limitation to intelligently designing improvements to these materials.

The majority of existing surface techniques (AES, XPS, UPS, SERS, DRIFTS, etc.) rely on the interaction between an energy beam and a solid. The nature of the interaction between the beam and the solid determines the thickness of the "surface" investigated with the particular technique. Surface thicknesses vary from near millimeters in XPS to near nanometers in AES [1]. If two separate beam techniques sample from two different "surfaces" of the same material, they could give two different results for the surface composition of any particular material analyzed. While this dif-

Abbreviations: AES, auger electron spectroscopy; XPS, X-ray photoelectron spectroscopy; UPS, ultraviolet photoelectron spectroscopy; SERS, surface-enchanced Raman spectroscopy; DRIFTS, diffuse reflectance infrared fourier transform spectroscopy; XAS, X-ray absorbance spectroscopy; EELS, electron energy loss spectroscopy; AFM, atomic force microscopy; STM, scanning tunneling microscopy; ESCA, electron spectroscopy for chemical analysis

* Corresponding author. Present address: 26463 Solon Road #303, Oakwood Village, OH 44146, USA.
E-mail address: tornado40@hotmail.com (B.C. Peebles).

0021-9673/$ – see front matter © 2004 Elsevier B.V. All rights reserved.
doi:10.1016/j.chroma.2003.12.065

ference exists whether the sample has a flat surface or is a fine powder, it is particularly noticeable for powders. Energy beams impinge both the top and sides of powders; whereas on a material that has a flat surface, the beam impinges the top of the sample only.

Recent research has accounted for the differences between direct and oblique impact of an energy beam on a particle surface. Sánchez-López and Fernández [2] compared XPS (i.e., surface composition) data to XAS and EELS (i.e., total composition) data for nanometer sized aluminum particles with a thin alumina coating. They explained their results with a model that accounts for the fact that an X-ray beam that hits the side of a particle samples more of the alumina region than an X-ray beam that hits the top of the particle.

The atomic microscopies, AFM and STM, suffer from a slightly different problem when analyzing powders. Inherently, both techniques only sample the top layer of atoms on a material. To do this effectively; however, the surface must be nearly flat and parallel to the microscope stage. These conditions can be difficult to obtain with fine powders.

This discrepancy between information obtainable with existing surface techniques and information desired from surface techniques could be solved by approaching the problem from a completely new direction. Existing surface analysis techniques typically examine physical phenomena, such as interaction with an energy beam. Often, the analytical chemist would also like to find information about the surface of the sample that might be based on chemical properties that are different from those found in the bulk. This would require new methods to investigate the surface composition of powders, based on chemical phenomena rather than physical phenomena.

The surface analysis technique described in this paper uses a selective dissolution process to gather its information. As a powder dissolves, it dissolves from the surface inward. The longer a powder has been dissolving, the more of the interior has been dissolved. The HPLC surface analysis technique determines the correct conditions to dissolve the surface without dissolving the bulk. Once surface species are separated from the bulk, they can be determined using existing techniques. Since the HPLC surface analysis technique relies upon the chemical process of dissolution, it inherently reveals information about the chemical behavior of the surface.

There are two distinct steps to this new technique. In the first step, a solvent system is found in which the powder is only sparingly soluble. In the second step, the powder is placed in this solvent system and the solvent is analyzed after having been exposed to the powder. Any species that appear in the solvent after having been exposed to the powder must have come from the surface of the powder. Since the solvent system was chosen to not dissolve the bulk powder, the interior should not have appreciably dissolved. The solvent should have desorbed any material present on the powder's surface and taken only a negligible amount of the bulk. This method is not new, but its application to powders may be. Ernstsson et al. used desorption from quartz surfaces by a liquid phase to investigate the nature of the interface between quartz and the absorbed species [3]. Unlike that study in which ESCA was used to analyze the quartz before and after desorption, the liquid phase was analyzed directly in their experiments to find the surface composition.

The approach explored in this paper uses gradient HPLC for both steps. The sample powder is loaded into a chamber on the pump side of a column. As the eluent composition changes, analytes will desorb or dissolve from the particles. Membranes in the chamber keep the particles from entering the column. The column then retains the analytes for subsequent separation with a different eluent.

In principle, this technique could be used to investigate non-ionic species as well as ionic species. The proper eluent system and detector would determine which surface species are analyzed in a particular investigation. This paper investigates the feasibility of using chelation ion chromatography to determine the presence of transition metal ions on the surface of iron(III) and copper(II) oxides.

Many powders of interest are transition metal oxides. For such materials, decreasing the acid content of the eluent will generally decrease the solubility of the bulk powder. With a sufficiently low acid content, ideally, the bulk powder will not dissolve. Any species present in the solution passing through the detector must be from the powder's surface. The key to analyzing the powder surface in the specific application presented here is the determination of the minimum pH conditions in which the iron(III) and copper(II) oxide surfaces will not dissolve.

2. Experimental

2.1. Reagents

Samples of iron(III) oxide (99.6%, ACS) were obtained from J.T. Baker (Phillipsburg, NJ, USA). Copper(II) oxide (ACS) was obtained from Mallinckrodt (New York, NY, USA).

The media used to confine the solid samples were cleaned thoroughly before analyses in an aqueous solution of ethylene diamine tetraacetic acid (EDTA) buffered by ammonia and ammonium chloride. EDTA (100.4% assay, ACS) was obtained from Mallinckrodt (Paris, KY, USA). Aqueous ammonia (15.2 M, ACS) was obtained from Fisher (Fairlawn, NJ, USA). Ammonium chloride (ACS) was also obtained from Fisher.

Hydrochloric acid solutions were used in all surface dissolution methods. Hydrochloric acid (12 M, trace metal grade, ACS) was also obtained by Fisher.

The water used to make all solutions had been filtered through activated charcoal and through a reverse osmosis unit. The resulting water was better than American Society for Testing and Materials (ASTM) Type II, with resistivities >14 MΩ cm.

The eluent for transition metal separations was prepared as specified by the column manufacturer. Oxalic acid

and tetramethylammonium hydroxide (>99%, ACS) were obtained from Fisher. Potassium hydroxide (85%) was obtained from Spectrum (New Brunswick, NJ, USA).

The post-column reagent for transition metal determination was also prepared as specified by Dionex. 4-(2-Pyridylazo)resorcinol (PAR, >99%, ACS) was obtained from Aldrich (Milwaukee, WI, USA). Dimethylaminoethanol (99%, ACS) was obtained from Acros (NJ, USA), and sodium bicarbonate (100.2% assay, ACS) was obtained from Fisher.

High-purity mass spectroscopy standards were used to duplicate the solution used by Dionex to test the CS5A column. Standards of lead(II), copper(II), cadmium(II), cobalt(II), zinc(II), and nickel(II), 1000 mg/l in 3% (v/v) aqueous nitric acid, were obtained from SCP Science (Champlain, NY, USA).

2.2. Instrumentation

A Dionex (Sunnyvale, CA, USA) GP40 gradient pump delivered all eluents to the sample loop or chamber through a Rheodyne (Coati, CA, USA) 9125 injection valve. The sample chamber was connected to the injection valve in place of a sample loop for experiments in which powdered samples would be dissolved. A Dionex CS5A 4 mm column was used in tests determining the feasibility of separating surface analytes. A helium-driven Dionex PC10 Postcolumn Reagent Delivery System delivered the post-column reagent through a mixing tee to the effluent. The PAR–metal complex was detected by absorbance with a Dionex AD20 absorbance detector. All iron(III) and copper(II) oxide samples were weighed to the nearest microgram with a Mettler-Toledo (Greifensee, Switzerland) MX-5 microgram balance. The approximate size distribution of copper(II) oxide particles was determined using an ATM (Milwaukee, WI, USA) L3P sonic sifter fitted with ATM 5, 10, 15, and 25 μm pore diameter electroformed mesh sieves.

A Dionex high-pressure in-line filter housing (P/N 44105) was modified to serve as the sample chamber (Fig. 1). The sintered polymer filter was removed and replaced by a Teflon cylinder, sized to exactly fill the filter cavity and hollowed to allow the eluent stream to pass through. The Teflon rods were obtained from McMaster Carr (Elmhurst, IL, USA) and machined into the necessary parts. The sample was placed between two Celgard (Charlotte, NC, USA) 3501 polyethylene membranes that confined sample particles while allowing dissolved species to pass through. Spectra Mesh (Los Angeles, CA, USA) F 74 μm ethylene–tetrafluoroethylene copolymer woven mesh filter screens were used to support the membranes and prevent membrane rupture under pressure. Although not shown by Fig. 1, the sample, membranes, and support screens were flattened firmly between the Teflon cylinder and the male end of the inline filter housing. The threads that held the male and female filter housing components together were removed to allow the pieces to fit without any twisting motion. In place of the threads, two stainless steel compression plates provided enough compression to seal the sample chamber. The plates were fastened together by four bolts, tightened uniformly to 5.4 Nm with a torque wrench.

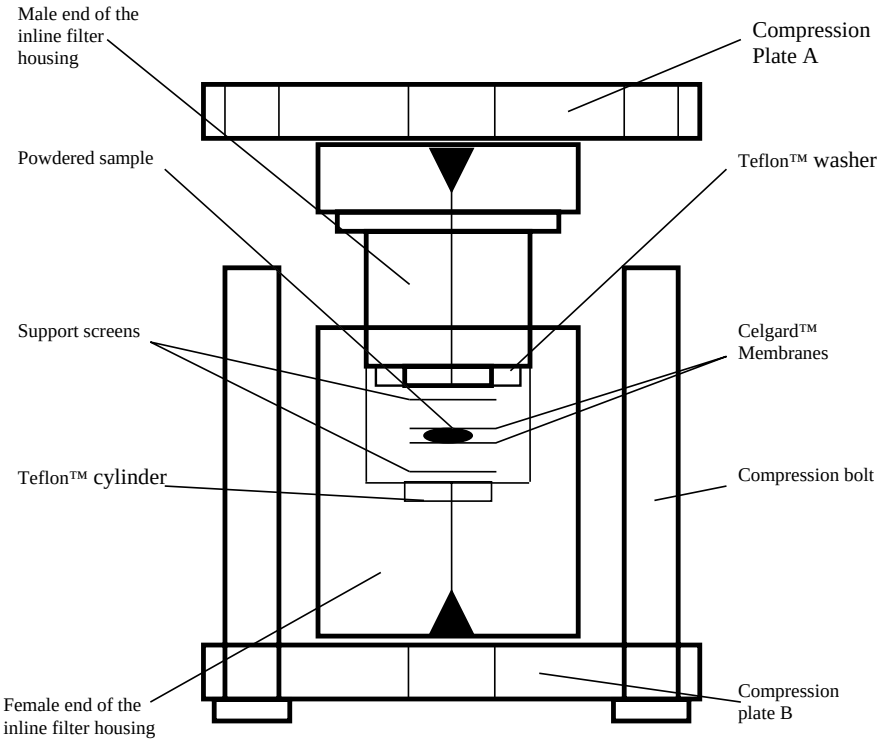

Fig. 1. The sample chamber (expanded to show contents).

2.3. Methods to optimize surface dissolution

Before all analyses, the Celgard membranes and the support screens were thoroughly cleaned to eliminate any potentially interfering transition metals. Membranes and screens were shaken and soaked in glass bottles for 15 min in 15 mM EDTA, buffered to pH 10 with aqueous ammonia and ammonium chloride. The screens and membranes were then shaken in each of the two glass bottles of deionized water and left for 5 min.

The post-column reagent delivery system was adjusted to deliver the PAR solution at 0.6 ml/min for detection of transition metals. The PAR–metal complex was detected by absorbance at 520 nm, at the highest intensity visible lamp setting on the AD20. Absorbance values were recorded every second by Dionex PeakNet software. The raw chromatographic data were imported into Microsoft Excel for detailed analysis.

Before the pH was found at which the surface of the iron(III) oxide sample dissolved, it was necessary to determine the time between the eluent leaving the pump and arriving at the sample chamber. This "lag time" between the gradient pump and the sample chamber was measured as the time between the introduction of hydrochloric acid to the eluent and the first detection of dissolved species from the loaded sample chamber. The gradient pump was programmed to purge the system for 5.0 min with deionized water, expose the sample to eluent at pH 3.0 in hydrochloric acid, and purge the system again for 2.0 min with deionized water. The experiment ran at 1.0 ml/min with no column.

The highest eluent pH that would dissolve the iron(III) oxide sample dissolved was found using the eluent profile shown in Table 1. Again, no column was used. The previously determined lag time was subtracted from the time when species were first detected, to give the method time at which the eluent leaving the gradient pump was sufficiently acidic to start dissolution. Solvent conditions at that method time were found by comparison with the eluent profile.

Quantitative surface dissolution experiments were designed to test the reproducibility of sample dissolution. Copper(II) oxide was used rather than iron(III) oxide because copper(II) oxide's higher solubility in hydrochloric acid was found to produce more meaningful dissolution curves. The method used in these experiments purged the system for 3.0 min with deionized water and then delivered hydrochloric acid at a nominal pH of 3.0 to dissolve a portion of the sample. Another 3.0 min deionized water purge was used to flush the system for the next experiment. The method was run at 1.0 ml/min without a column.

Table 1
The eluent profile used to approximate the conditions for optimal surface dissolution of iron(III) oxide between pH 7.0 and 3.0

Method time (min)	Water (%)	0.001 M hydrochloric acid (%)	Nominal eluent pH
Initial	100	0	7.0
0.00	100	0	7.0
5.0	100	0	7.0
6.0	99.9	0.1	6.0
7.0	99.9	0.1	6.0
9.0	99.0	1	5.0
15	90	10	4.0
21	0	100	3.0
22	0	100	3.0
27	End	End	End

All pH changes between consecutive time values are linear in hydrochloric acid concentration.

The physical properties of the copper(II) oxide samples and the dissolution curves obtained in the quantitative dissolution experiments were used to develop a more comprehensive model of surface dissolution. The model was developed to support claims that surface and bulk dissolution have been separately observed, lending credence to the feasibility of surface characterization without simultaneous bulk analysis. According to this model, the theoretical weight of a monolayer of the sample should agree with the mass of the sample determined to have dissolved in a given region of the dissolution curve. The mass of the theoretical surface monolayer of copper atoms per mass of sample was calculated from the approximate surface area distribution of the sample and the crystal structure of copper(II) oxide. The sample was sifted at amplitude setting 5 with sonic pulses for 30 min to obtain the particle size distribution necessary for these calculations. The weight of the sample's surface monolayer was compared with the experimentally determined weight of copper that was thought to be from the surface, to strengthen claims that surface dissolution and bulk dissolution are distinct processes.

Liquid injections of transition metal standards were used to test whether methods can be developed using existing equipment to first dissolve the surface of a metal oxide sample, and then separate its components by ion chromatography. A multicomponent standard consisting of 3 mg/l lead(II), 0.5 mg/l copper(II), 3 mg/l cadmium, 0.5 mg/l cobalt(II), 1 mg/l zinc(II), and 2 mg/l nickel(II) was prepared from 1000 mg/l mass spectrometry standards. The standard was injected through a 100 μl sample loop instead of through the sample chamber that was previously used. A 5.0 min water purge followed by 5.0 min of exposure to pH 4.0 hydrochloric acid eluent was used to test the column's ability to retain the components in the standard under both neutral and moderately low-pH conditions in hydrochloric acid. This method simulated conditions that would be used to dissolve the surface of a powdered metal oxide prior to separation.

Immediately afterwards, the eluent was changed to elute and separate the species previously loaded on the column. The new eluent was an aqueous solution of 80 mM oxalic acid, 100 mM tetramethylammonium hydroxide, and 50 mM potassium hydroxide, as suggested by the column manufacturer. The 15 min isocratic separation method was run at 1.2 ml/min with the injection valve in the "load" position to bypass the sample loop. This would be necessary in a solid surface analysis to prevent the bulk material from dissolving and interfering with the surface characterization.

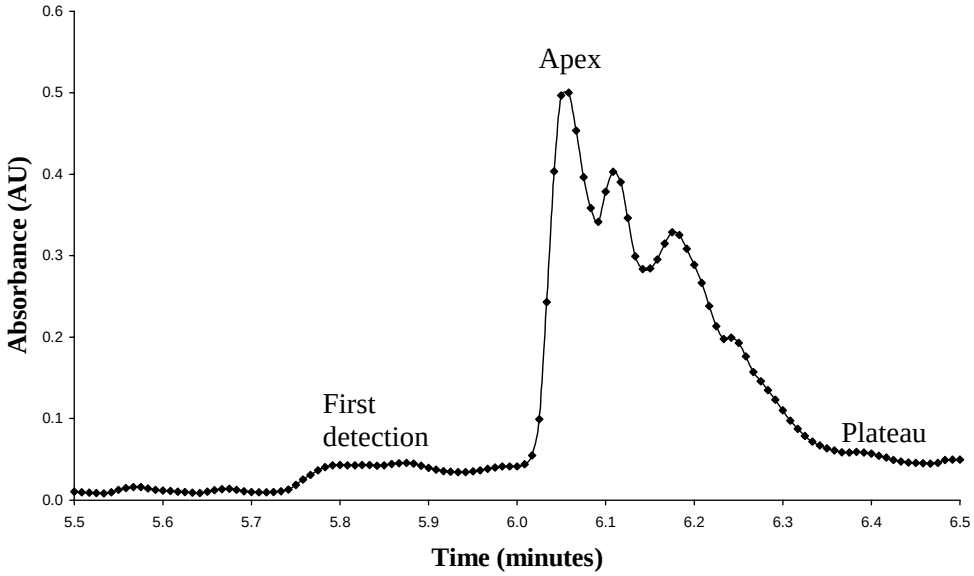

Fig. 2. Determination of lagtime at a constant pH 3.

3. Results and discussion

3.1. The mechanical performance of the sample chamber

The bolted compression plates provided sufficient compression to seal the chamber. The sample chamber rarely leaked when the compression bolts were tightened to 5.4 Nm. On rare occasions when the chamber did leak, the run was discarded as an anomaly. While using the sample chamber in experiments without a column, the eluent pressure ranged from 2068 to 3447 kPa. The sample chamber has withstood eluent pressures up to 15,860 kPa, approximately twice the pressure expected with the use of a 4 mm transition metal separation column, without leaking.

3.2. Determination of instrument lag time

The lag time between the pump and the detector is displayed graphically in Fig. 2. The gradient pump delivered hydrochloric acid after 5.0 min elapsed. The first traces of dissolved sample appeared after 5.7 min, shown by the initial modest absorbance increase from the baseline level. Subtracting the time of acid introduction from the time at which dissolved sample was first detected gave the lag time between the pump and the detector, 0.7 min.

The lag time experiment also provided the first evidence that surface and bulk dissolution are distinct processes. The sudden signal increase shortly after 6.0 min is possibly due to the beginning of surface material dissolution in low-pH conditions. The dissolution later became less predictable, as shown by the irregular dissolution curve. The authors suggest that the subsequent irregularity in the dissolution curve was caused by the bulk breaking into smaller particles as it dissolved. As the curve became unpredictable, the eluent pressure sometimes increased, indicating that small sample particles were plugging the membrane's pores until the high pressure alarm on the gradient pump sounded. When the pressure did not rise to a level that tripped the alarm, however, the absorbance signal fell from its apex to a near-baseline plateau level as shown in Fig. 2 although the solid had not completely dissolved. This indicated a rapid dissolution process in the beginning as the surface was first exposed to acidic conditions, but a slower process as the bulk dissolved. These results suggested that the bulk was not as easily or as predictably dissolved in hydrochloric acid at pH 3.0 as was the surface. It follows that the surface could be dissolved separately from the bulk under the right conditions. By visual estimate, most of the sample remained in the sample chamber after this determination.

3.3. Optimization of eluent conditions using a pH gradient

Once the lag time between the pump and the detector was determined, the best conditions for surface dissolution were found using the eluent profile with the pH gradient previously described. The lag time of the instrument was determined to be 0.7 min in the earlier experiment. The time of first detection was 8.1 min, shown graphically on Fig. 3. Therefore, eluent that was sufficiently acidic to dissolve the surface of the sample left the gradient pump when 7.4 min had elapsed. Interpolation between the two nearest known nominal pH values at 7.0 and 9.0 min on the eluent profile showed that the surface of the iron(III) oxide sample began to dissolve at a nominal pH of 5.6.

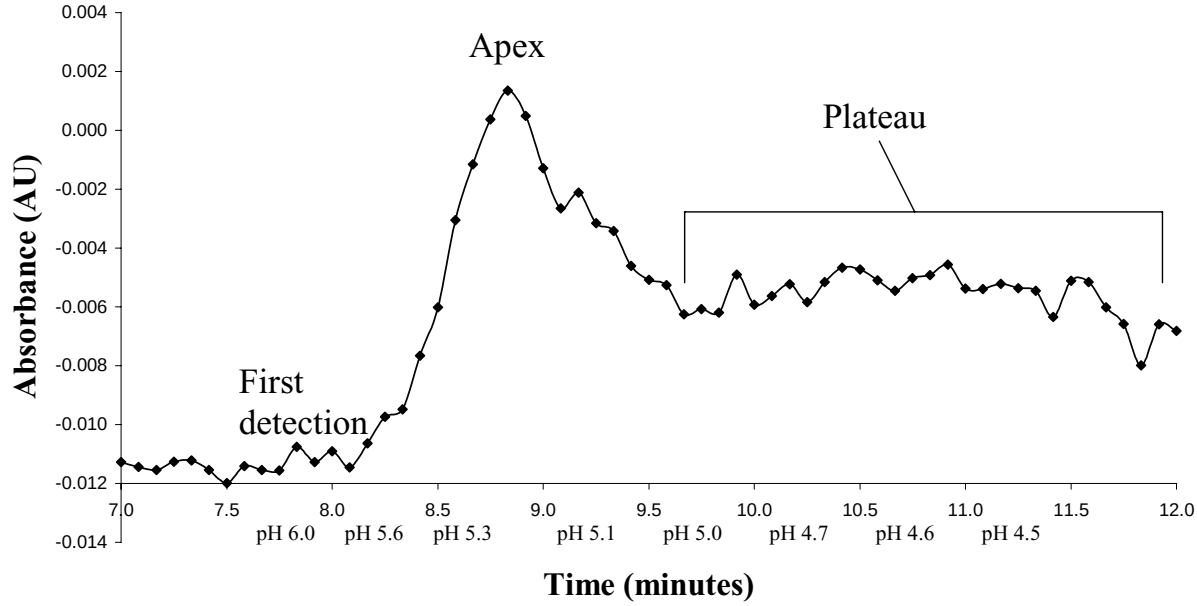

Fig. 3. Approximation of pH conditions for optimal surface dissolution of iron(III) oxide using a pH gradient from 7.0 to 3.0.

3.4. Qualitative observation of the surface dissolution of copper(II) oxide

The results of dissolution experiments with copper(II) oxide at a constant pH of 3.0 showed the reproducibility of the dissolution process that occurred in the sample chamber. More than 20 consecutive, similar dissolution curves have been obtained with copper(II) oxide in repeated experiments with the described HPLC methods. Comparably shaped dissolution curves have also been obtained in other experiments [4]. Fig. 4 shows the typical dissolution curve of copper(II) oxide at a constant nominal pH of 3.0. The region on the curve between the start of the method and the beginning of the surface dissolution is referred to as "region 1" in this paper. The small peak near the start of the method shows the dissolution of a yet unidentified species in deionized water. Although the peak was characteristic of the effect of an air bubble from the sample chamber reaching the detector, this is unlikely since the detector effluent visibly reddened at the same time. In "region 2," the curve reached its apex and

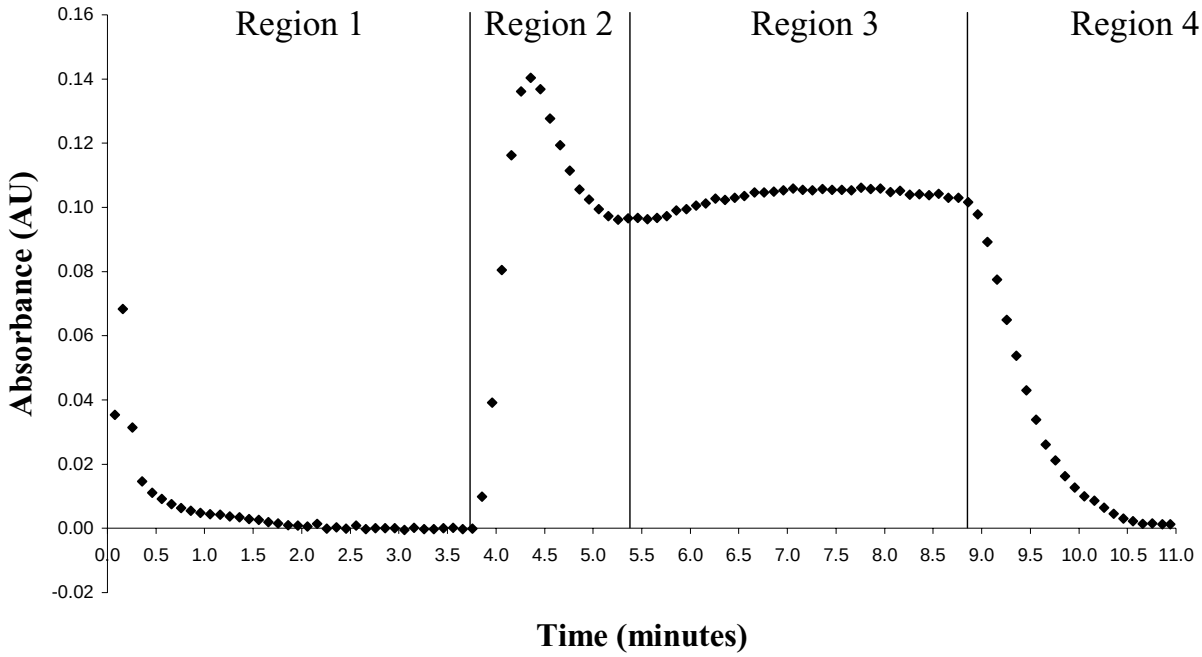

Fig. 4. The typical CuO dissolution curve at constant pH 3.

Table 2
Descriptive statistics of signal area/mass from three consecutive copper(II) oxide dissolution trials on the same day

	Area/mass ratios calculated by regions (g^{-1})				
Sample mass (μg)	Total signal area	Total	Region 1	Region 2	Region 3 + 4
835	1.82	2180	60.4	448	1670
852	1.72	2020	68.0	424	1520
946	1.62	1710	72.5	391	1480
S.D.		230	6.1	29	100
R.S.D. (%)		12	9.1	6.8	6.4

3.0 min deionized water purge, 5.0 min in hydrochloric acid of pH 3.0, 3.0 min deionized water purge.

declined to lower value. This is interpreted as the surface having completely dissolved. In "region 3", the absorbance equilibrated to a plateau value. This is interpreted as the more gradual dissolution of the bulk. If the interpretation of region 3 is correct, this plateau would decrease as the bulk dissolved, theoretically until no sample would remain. This decline was not observed, however, due to the final deionized water purge. "Region 4" shows the rapid decrease in absorbance as dissolved sample material was purged from the system with deionized water.

3.5. Quantitative analyses of the reproducibility of copper(II) oxide dissolution

The reproducibility of the dissolution curve shape allowed a more quantitative analysis of the dissolution process. Three runs with similar sample masses were performed on the same day and analyzed for descriptive statistics. The descriptive statistics that indicated experiment reproducibility were detection area per sample weight for each region. These are shown on Table 2. Region 2 warrants special attention, since it has been attributed to the surface dissolution phenomenon. The 6.8% R.S.D. in detection area per sample weight for region 2 between the three experiments suggests that the region attributed to surface dissolution is reproducible, which is critical for the success of HPLC surface analysis.

3.6. Explaining the features of copper(II) oxide dissolution curves in terms of separate surface and bulk phenomena

A simple model was developed to test the assignment of region 2 as being due to surface dissolution. The weight of copper in one monolayer at the surface of the sample was compared to the experimentally determined weight of copper that was dissolved in the time frame corresponding to region 2 on the dissolution curve.

To calculate the specific surface area of the sample, its approximate particle size distribution was found by sonic sifting. Results of the sifting experiment are shown on Table 3. By approximating the particles to be spherical, their weighted average specific surface area was found to be 0.246 m^2/g.

Table 3
Experimental size distribution of sample particles of copper(II) oxide

Diameter (μm)	Fraction mass	Total (%)
<5	0.0914	4.50
5–14	0.335	16.5
15–24	0.327	16.1
25–100	1.28	62.9

2.03 g sample, sifted and pulsed for 30 min, amplitude setting 5.

The density of copper(II) oxide [5], its centered monoclinic crystal structure [6], its molecular mass, and the atomic mass of copper were used to calculate the theoretical weight of the surface copper monolayer of the sample, assuming that the crystal lattice terminates with copper atoms exposed. Since the model of surface phenomena is meant only to strengthen evidence in favor of the dissolution model discussed in this paper, approximating the copper(II) oxide crystal lattice to be body-centered cubic for simplicity does not diminish the validity of the calculations. The mass of copper atoms on the exposed face of one body-centered cubic unit cell is 1.06×10^{-16} μg. Combining this value with the specific surface area value previously determined in sonic sifting experiments, the mass of the surface monolayer per mass of sample was calculated to be 3.40×10^{-4}.

The same data previously used to gather descriptive statistics on the dissolution were employed to find the weight of copper that dissolved in the time frame corresponding to region 2 on the dissolution curves. A calibration curve was obtained, relating the detection area to the mass of copper(II) from three liquid standards that were injected into a 100 μl injection sample loop instead of the sample chamber. Concentrations of copper(II) in the standards were 0.1, 0.3, and 0.5 mg/l. The calibration equation relating detection area (y) to the weight of copper injected (x) was found to be $y = 0.139x + 0.0162$, with $R^2 = 0.995$.

If the dissolution model is accurate and region 2 results from surface phenomena, the mass of copper detected in region 2 should be comparable to the theoretical mass of copper on the surface, for each sample. The comparison between the actual dissolved mass and the theoretical surface mass is shown in Table 4. Although the mass of copper detected is approximately 10 times the theoretical mass of copper on

Table 4
Comparison of the theoretical mass of the monolayer of copper atoms at the surface with the actual mass of copper found to have dissolved in region 2 of the dissolution curve: data from three consecutive trials on the same day

Sample mass (μg)	Approximate surface area ($m^2 \times 10^{-4}$)	Theoretical monolayer mass (μg)	Actual mass of Cu dissolved in region 2 (μg)
835	2.05	0.284	2.58
852	2.09	0.290	2.49
946	2.32	0.320	2.23

3.0 min deionized water purge, 5.0 min in hydrochloric acid of pH 3.0, 3.0 min deionized water purge.

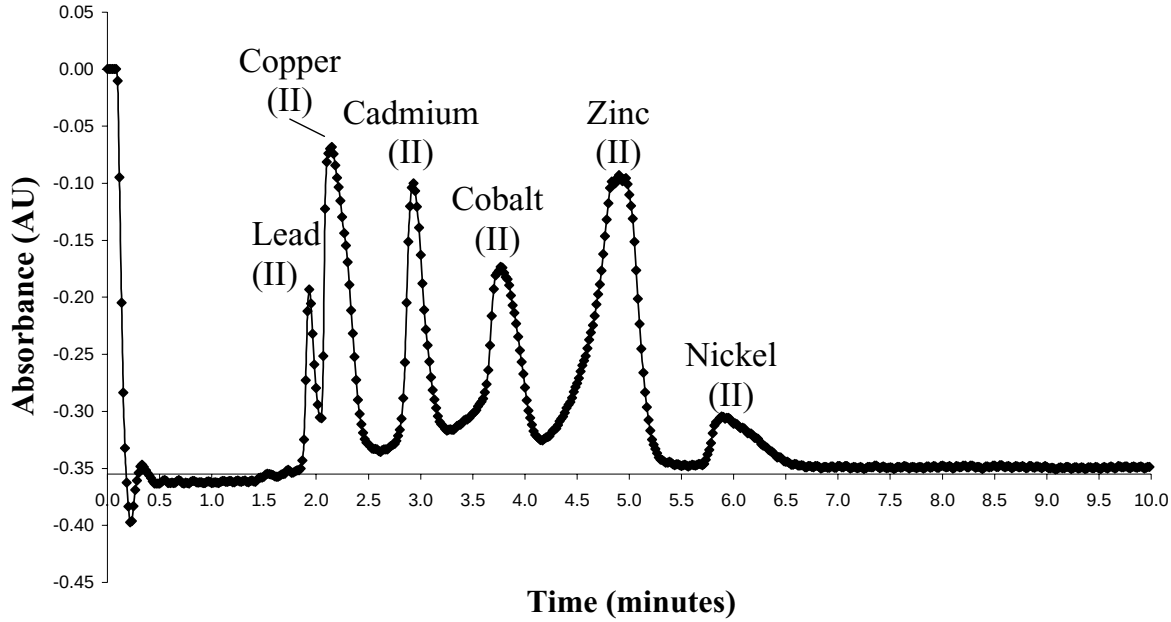

Fig. 5. Separation of the test solution on the CS5A column, after running the dissolution method.

the surface of the sample, the similarity is still believed to be supportive of the claim that region 2 on the dissolution curves can be attributed to surface dissolution. The theoretical values assumed that the particles were spherical. If they were not, the surface to mass ratio would increase, increasing the theoretical mass of the surface. Similarly, if the copper(II) oxide particles contained pores, the mass of the surface would increase. Additionally, the theoretical mass would increase if the portion of particle that is chemically different from the bulk penetrated more than one monolayer into the sample. The theoretical value, therefore, is expected to be lower than the experimental value due to the assumptions of the model. For example, if the particles were actually rods with an aspect ratio of 4 and the same volume as of the sphere, the theoretical surface mass would increase by nearly 40%. The particle morphology of the copper(II) oxide sample has not been determined.

3.7. Tests of the column's ability to support methods that would strip the surface of a metal oxide powder and separate its components

To support the hypothesis that a procedure that would first dissolve the surface of a metal oxide powder and then separate transition metal species on the surface is technically feasible with existing apparatus, the Dionex CS5A column's ability to support such a proposed procedure was verified.

When a solution of lead(II), copper(II), cadmium(II), cobalt(II), zinc(II), and nickel(II) was injected and the dissolution profile was run at a nominal pH of 4.0, a flat baseline and the absence of analyte peaks indicated that the column retained the analytes.

When the eluent was changed to elute and separate the analytes, the Dionex CS5A column proved to be effective. The resulting chromatogram from the dissolution–separation feasibility experiment is shown in Fig. 5. All components are identifiable and quantifiable. This supports the hypothesis that a procedure that would first dissolve the surface of a metal oxide powder and then separate the transition metal species from the surface is technically feasible with existing equipment.

4. Conclusions

Results suggest that the surfaces of iron(III) and copper(II) oxide powders dissolve differently from the bulk. That this difference can be seen using HPLC warrants further investigation of this technique: it follows that the dissolution of only the surface may be possible under the right conditions, allowing analysis of constituents on that surface.

A method was successfully executed to determine the conditions at which the surface of a sample of iron(III) oxide will dissolve. Experiments with samples of iron(III) oxide demonstrated that a gradient pump can be used to determine the point at which the sample's surface begins to dissolve but the bulk remains mostly intact.

Qualitative observations and later calculations show that the dissolution of copper(II) oxide at a constant nominal pH of 3.0 is reproducible using apparatus and methods described in this paper. Each dissolution curve was split into the same four distinct regions that seemed to display separate surface and bulk phenomena. The most important region in the focus of this paper, the region attributed to surface phenomena, displayed a relative standard deviation of detection area to

sample mass of 6.8%. Assuming that region 2 on the dissolution curves can be attributed to surface phenomena, this value shows that surface dissolution is reproducible.

The theoretical mass of the surface monolayer of copper atoms on copper(II) oxide samples is comparable to the actual mass of dissolved material calculated from the region of the dissolution curves that has been attributed to surface dissolution, when simplifying assumptions about the shape of the particles are considered. Such agreement strengthens the hypothesis that the surfaces of the copper(II) oxide samples used in these experiments are chemically different from their bulk, allowing dissolution and analysis of only the surface.

To determine the feasibility of surface analysis by HPLC using existing apparatus, a set of methods was tested that would dissolve the surface of a metal oxide powder and later separate its constituents. The chromatograms obtained in these experiments showed that the column retained the analyte under conditions that would strip the surface of a metal oxide powder, then eluted and separated the constituents of the analyte during the separation method. These results show that methods to strip and separate the surfaces of metal oxide powders would work with existing equipment.

Future work with this HPLC surface analysis technique will verify its feasibility by examining different particle size fractions of the same powdered sample. Surface contaminants on any given powdered sample would be expected to have the same area concentration regardless of the particle size; however, the different particle sizes will have different mass concentrations of the contaminants. Therefore, if the powder sample is sieved into several fractions and then analyzed, there should be a predictable difference in contaminant concentration between fractions, depending on the particle size of each fraction. This general approach of evaluating powder analysis with several particle sizes has been done with XRF [7] and DRIFTS [8], and could easily be attempted using HPLC surface characterization techniques.

Acknowledgements

The authors would like to thank the Kresge Foundation for providing funding for the purchase of HPLC equipment, and the Department of Chemistry, John Carroll University, for general research funding and facilities.

References

[1] K.A. Rubinson, J.F. Rubinson, Contemporary Instrumental Analysis, Prentice-Hall, Upper Saddle River, NJ, 2000, p. 408.
[2] J.C. Sánchez-López, A. Fernández, Surf. Interface Anal. 26 (1998) 1016.
[3] M. Ernstsson, P.M. Claesson, S.Y. Shao, Surf. Interface Anal. 27 (1999) 915.
[4] M. Setter, E. Newbould, John Carroll University, Cleveland, OH, 2003, in preparation.
[5] D.R. Lide (Editor-in-chief), CRC Handbook of Chemistry and Physics, 81st ed., CRC Press, Boca Raton, FL, Section 4, 2000, p. 58.
[6] Swanson, Tatge, NBS Circular #539 (I), p. 49 (1953). Powder Diffraction Data, in: H.E. Swanson, S.J. Carmel (Eds.), National Bureau of Standards, Swarthmore, PA, 1976, p.29, card #5–661.
[7] T. Horváth, V. Szilágyi, Z. Hartyáni, Microchem. J. 67 (2000) 53.
[8] L. Tremblay, J.P. Gagné, Anal. Chem 74 (2002) 2985.